

## Study The Effect Of Different Common Beam Sections Having A Constant Cross Sectional Area On The Critical Buckling Load

**Dr. Abdul-Wahab Hassan Khuder**

Assistant Professor

Technical College-Baghdad

[akhuder@yahoo.com](mailto:akhuder@yahoo.com)

**Sabah Khammass Hussein**

Lecturer

Technical College-Baghdad

[Sabah.Kh1974@yahoo.com](mailto:Sabah.Kh1974@yahoo.com)

**Ammar Azeez Mahdi**

Assistant Lecturer

Technical College-Baghdad

[Ammaraz83@yahoo.com](mailto:Ammaraz83@yahoo.com)

### SUMMARY:

A simply supported beam is used to calculate the critical buckling load. A common beam sections with constant cross sectional area are used to analyze the results using ANSYS11 program which gives a good results as comparing with the theoretical equation. The critical buckling load depends on the shape and dimensions of beam section which has constant cross sectional area. It observed that the critical buckling load is higher with a wide range of width for thinner hollow rectangular-section than the thicker section and lower for ( I, T & L-sections). Changing the width or thickness for U & Z-sections gave a small effect on the critical buckling load. Increasing the thickness of hollow circle beam section gives a decreasing in the critical buckling load. The last beam section gives a higher critical buckling load as comparing with solid circle section of the same cross sectional area. The same phenomenon is found for hollow rectangular-section as comparing with the solid section.

**Keywords:** A simply supported beam, Critical buckling load.

### المستخلص:

تم استخدام عتبة ذات ارتكاز البسيط من الطرفين لحساب حمل الأنبيعا الحرج. تم استخدام المقاطع الشائعة من العتبات بثبوت المساحة لتحليل النتائج باستخدام برنامج (ANSYS11) والذي أعطى نتائج جيدة مقارنة مع المعادلة النظرية. حمل الأنبيعا الحرج يعتمد على شكل وأبعاد مقطع العتبة الذي يمتلك مساحة ثابتة.

لوحظ من النتائج أن حمل الأنبعاث الحرج يكون عالي بمدى واسع للمقطع المستطيل المجوف النحيف مقارنة مع المقطع السميك وتكون قليلة في المقاطع ذات الأشكال (I,T&L). تغيير عرض أو سمك المقطع ذات الأشكال (U&Z) أعطى تأثير قليل على حمل الأنبعاث الحرج. زيادة سمك مقطع العتبة الدائري المجوف يعطي نقصان في حمل الأنبعاث الحرج وأعطى حمل أنبعاث حرج عالي مقارنة مع المقطع الدائري الصلب لنفس مساحة المقطع. نفس الظاهرة الأخيرة لوحظت في المقطع المستطيل المجوف مقارنة مع الصلب.

## 1. Introduction:

Euler was the first who studied for engineering applications important problem of buckling arising in a simple, monolithic beam loaded axially by a concentrated load. It has been shown from two solutions of the problem due to Timoshenko theory; the elastic foundation increases the critical buckling load of the beam. Starting from the previous classical results, a mechanism to enhance the buckling strength of a cantilevered beam is investigated. In the place of a single, one-element, monolithic cross-section, the use of a bundle of more than one, similar or not, single cross-sections, placed with parallel axes, and staying in free contact along their adjacent boundaries, is proposed [1].

The buckling behavior of an I-beam under combined axial and horizontal loading is examined. It is shown that the actual application location of the axial loading governs the buckling behavior of the long I-beam. Theoretical formulation is developed to determine the critical buckling load for such combined loading configuration from the elastic static theory. Both, the beam deflection theoretical model and the critical load capacity are derived for this combined loading condition. The Finite Element Analysis (FEA) is utilized to apply the axial load on the beam at various configuration locations and it is shown that this application location determines the buckling behavior and the critical load of the buckling of the I-beam [2]. Tapered I-beams can carry a maximum bending moment at a single location while in the rest of the member the moment carrying capacity is considerably lower. Numerous researchers have focused on the investigation of the elastic behavior of tapered I-beams and many theoretical findings have been incorporated into the current specifications. The elastic critical moment is used for determining the design strength against lateral-torsional buckling (LTB) of I-beams with uniform cross-section and a number of coefficients is employed accounting for the boundary conditions, the cross-sectional geometry and the type of transverse loading, while no detailed information is given regarding non-uniform members. Modification factors of the elastic critical moment with reference to the mean cross-section are given for various taper ratios. The approach presented here in can be very easily applied for the design of tapered beams against lateral-torsional buckling [3].

The lateral-torsional buckling of composite strip and I-beams is considered. The geometrically exact governing equations are simplified by consistently regarding certain configuration parameters as small. The assumption that these parameters are indeed small is equivalent to the assumption that the square of the maximum prebuckling cross-sectional rotation due to bending is small compared to unity. The analysis takes into account various refinements of previously published results, elastic coupling, and the offset of the load from the centroid, and, of course, prebuckling deflections. The analysis is thereby reduced to a single fourth-order differential equation and boundary conditions, all of which are derivable from a corresponding energy expression. Using this comparison function, a formula for the buckling load as a function of the small parameters of the problem is found and validated. With certain exceptions regarding the load offset parameter; the formula provides results which agree quite well with the numerical solution of the exact equations as long as all the small parameters remain small. However, the load offset parameter always appears in the governing equations as multiplied by a ratio of stiffness, which can become large, especially for composite I-beams [4].

In steel construction the flange of a steel I-beam is usually coped to allow clearance at the connection. Local web buckling at the coped region may occur when the cope length is long and/or the cope depth is large, provided that lateral-torsional buckling of the beam is prevented. In order to verify such recommendation, an experimental and numerical investigation of coped I-beams with stiffeners at the coped region was conducted and reported. The local web buckling could not be prevented efficiently if only horizontal stiffeners were provided at the coped region. Both the test and the numerical results showed that the horizontal stiffeners at the cope displaced laterally due to gross web distortion. It was found that for cope depth to beam depth ratio  $(d/D) \geq 0.3$ , both horizontal and vertical stiffeners are required in order to prevent local web buckling at the cope region [5].

A method of identifying the buckling load of a beam-column is presented based on a technique named Multi-segment Integration technique. This method has been applied to a number of problems to ascertain its soundness and accuracy. The boundary conditions mean that, i) it is hinged at both ends; ii) it is fixed at both ends; and iii) it is fixed at one end and hinged at the other end. The results obtained by Finite Difference method are compared in order to determine the efficiency of this method [6].

In the present work, the lateral buckling response of a simply supported beam, subjected to a mid span concentrated load is thoroughly discussed. Assuming that the loss of stability occurs through divergence, we consider the equilibrium in a slightly bent configuration in which vertical and lateral deflections as well as angles of twist are developed. This state of equilibrium by a system of three differential equations with non-constant coefficients. Clearly, a closed form solution of the above system cannot be, in general, obtained. Therefore, one has to resort to approximate analytical solutions. Hence, an analytic approximate technique for solving the above system of differential equations is successfully employed [7]. The determination of the critical (elastic) level of loading is not only of theoretical, but also of practical importance, since in many current design codes, the design resistance of a beam against lateral buckling, even in the case of inelastic buckling, is based on the corresponding value of elastic buckling. The problems related to lateral buckling, results are obtained applying approximate procedures as well as finite element methods [8]. Approximate shape functions are also used, for establishing the post buckling behavior in cases of lateral (bending without axial force) [9], or lateral torsion buckling, [10, 11]. The effect of stacking sequences, fiber orientation angles, boundary condition and delamination numbers on the critical buckling loads of the laminated composite beams have been investigated analytically and numerically. Firstly, an analytical model is presented to take into consideration the reduction in stiffness of the beam due to the presence of the delamination in the beam. Then, two-dimensional finite element models for the composite beams having single/double middle delamination have been established by using contact element at ANSYS commercial program. A good agreement between theoretical and finite element results has been found. It is seen that the buckling loads vary with changing stacking sequences, orientation angles and boundary conditions. The results show that a reduction in the critical buckling loads occurs when delamination length increases. In the numerical analysis, the appropriate buckling load values of the laminated beams are obtained by using normal penalty stiffness that is chosen as elasticity modulus for contact elements in the delamination region [12]. This work deals with the lateral buckling of beams on which a concentrated load was applied through a bar subjected to a compressive force of constant direction. For the same cases of loading the problem of lateral buckling of beams under directed loading with the aid of finite element computer programs. Non-conservative problems are of paramount importance in modern structural design. The present paper deals with the lateral buckling and to calculate the critical buckling load. ANSYS11 program are using to analyze the results which gives a good results as comparing with the theoretical equation.

## 2. Theory of Columns Buckling (Euler Columns):

A assume a bar of length (L) loaded by a force (P) acting along the longitudinal beam axis on pinned end. As shown in Figure (1), the bar is bent in the positive y-direction, this required negative moment, and hence:

$$M = - Py \quad (1)$$

Where:

$M$ : moment (N.m).

$P$ : the applied load (N).

$y$ : moment arm (m).

If the bar should happen to bend in the negative y-direction a positive moment would results. The resulted moment can be written in the following equation:

$$EI \frac{d^2 y}{dx^2} = M \quad (2)$$

Where:

$E$ : modules of elasticity (N/m<sup>2</sup>).

$I$ : second moment of inertia (m<sup>4</sup>).

Sub Eq. (1) in Eq. (2):

$$\frac{d^2 y}{dx^2} = \frac{- Py}{EI} \quad (3)$$

or

$$\frac{d^2 y}{dx^2} + \frac{P}{EI} y = 0 \quad (4)$$

The solution of the above second order differential equation is as follows:

$$y = A \sin\left(\sqrt{\frac{P}{EI}}\right)x + B \cos\left(\sqrt{\frac{P}{EI}}\right)x \quad (5)$$

Where (A) and (B) are constants of integration and can be found from the boundary conditions.

In this work, the deflection is zero at both ends ( $x=0 \cdot L$ ). The first boundary conditions give ( $B=0$ ) and the other give:

$$A \sin\left(\sqrt{\frac{P}{EI}}\right)L = 0 \quad (6)$$

If  $A=0$ ; no buckling occurs, therefore:

$$\sin\left(\sqrt{\frac{P}{EI}}\right)L = 0 \quad (7)$$

Equation (7) is satisfied by:  $\sqrt{\frac{P}{EI}}L = n\pi$

Where:

n: is an integer.

Solving for  $n=1$  gives the critical load,  $P_{cr}$ :

$$P_{cr} = \frac{\pi^2 EI}{L^2} \quad (8)$$

Which called the "Euler column formula"

The critical applied stress,  $\sigma_{cr}$  (N/m<sup>2</sup>), is:

$$\sigma_{cr} = \frac{P_{cr}}{A} = \frac{\pi^2 EI}{AL^2} \quad (9)$$

The relation of radius of gyration, (k) for any cross sectional area is given by:

$$k = \sqrt{\frac{I}{A}} \quad (10)$$

Sub Eq. (10) in Eq. (9):

$$\sigma = \frac{P_{cr}}{A} = \frac{\pi^2 E}{(L/k)^2} = \frac{\pi^2 E}{S^2} \quad (11)$$

The term ( $S$ ) is known as the slenderness ratio. And the solution of Eq. (11) is called as a critical unit load. The buckling is occurred when the critical buckling stress is occurred below the yielding point of material where the “Euler column formula” is applicable. This occurred for long columns. The fail is occurs by compression for short columns. According to its length, the columns are classified as:

- (1) Short if  $S < 30$ .
- (2) Long if  $S > 120$ .
- (3) Intermediate  $120 > S > 30$ .

## 2-1. Principles Axis of Inertia:

Consider the cross sectional area of beam lies in the ( $y$ - $z$ ) plane, Figure (1). In Euler column formula, the moment of inertia is taken as the minimum moment of inertia either about the ( $y$ ) or ( $z$ )-axis for the beam section which has a moment of inertia ( $I_{yz}=0$ ). This is satisfied for the following beam section (used in this work):

- 1- Solid rectangular or square section.
- 2- Hollow rectangular or square section.
- 3- Ring or Hollow circular section.
- 4- Channel section.
- 5- T-section.
- 6- I-section.

The other type of beam section used in this work (L & Z-section) give a none zero value of ( $I_{yz} \neq 0$ ); where:

$$I_{yz} = A\bar{y}\bar{z} \quad (12)$$

There are two values of “ $\theta$ ” which locate the position of principle axes of inertia ( $Y,Z$ ) for a given cross sectional area:

$$\tan 2\theta = -\frac{2I_{yz}}{I_y - I_z} \quad (13)$$

The values of principle moment of inertia are given by:

$$I_Y = \frac{I_y + I_z}{2} + \sqrt{\left(\frac{I_z - I_y}{2}\right)^2 + I_{yz}^2} \quad (14)$$

$$I_Z = \frac{I_y + I_z}{2} - \sqrt{\left(\frac{I_z - I_y}{2}\right)^2 + I_{yz}^2} \quad (15)$$

Where:

$I_y, I_z$ : second moment of inertia about the (y & z-axis).

$I_Y, I_Z$ : principle moment of inertia about the principle axis (Y & Z-axis).

### 3. Finite Element Methods Using ANSYS11 Program:

#### 3-1. Material of Beam:

A carbon steel of type (Structural) is used for beam material. The yield stress is (250 Mpa), ultimate stress (400Mpa), Poisson's ratio (0.29) and have a young modulus of elasticity (E=200Gpa).

#### 3-2. Dimensions of Beam:

A constant cross sectional area is used for various beam section (common beam section). To ensure that the buckling is achieved and be applicable with Euler column formula, a suitable cross sectional area as compared with beam length must be choose to ensure that the buckling of beam within the yield region (satisfy Euler column formula). Hence the following beam dimensions are used for a different common beam cross section:

$A = 100 \text{ mm}^2$  (beam cross sectional area).

$L = 2000 \text{ mm}$  (beam length).

Where, the values of (S) in Eq. (11) is more than (120) for each of beam dimension used (long beam). The following beam cross sectional are used in this work:

- |                                |             |
|--------------------------------|-------------|
| 1- Hollow rectangular-section. | - Table (1) |
| 2- Channel-section.            | - Table (2) |
| 3- L-section.                  | - Table (3) |
| 4- T-section.                  | -Table (3)  |



- 5- I-section. - Table (4)  
 6- Z-section. -Table (4)  
 7- Hollow circle-section. - Table (5)  
 8- Solid circle-section. - Table (6)  
 9- Solid circle and square-section. - Table (6)

In each type of thin cross section, a finite number of thickness ( $t$ ), width ( $W_1$ ) and height ( $W_2$ ) are used such that the cross sectional area still constant ( $A=100 \text{ mm}^2$ ).

Hence, a three sets of dimensions used with thickness value ( $t = 1, 2, 3 \text{ mm}$ ) as shown in tables (1-4). For each thickness value, a wide range of sectional width is used. For example, in the first beam section, (Table-1), the width values are ( $W_1=5, 10, 15 \dots 50 \text{ mm}$ ) for the first set of thickness ( $t_1=1 \text{ mm}$ ). The other dimension ( $W_2$ ) is calculated such that the total cross section area equal to ( $A=100 \text{ mm}^2$ ). Where:

$$A=2W_1t+2(W_2-2t)*t=100 \text{ mm}^2$$

For the hollow circular section (Table-5), the values of thickness are ( $t=1, 2, 3, 4$  and  $5 \text{ mm}$ ). Hence the other dimensions are calculated such that the total cross section area is constant ( $A=100 \text{ mm}^2$ ). Table (6) gives the values of solid circle and square dimensions with the same above area. The moment of inertia ( $I_y, I_z, I_{yz}$ ), and other properties are calculated by ANSYS11 program for each beam section.

### 3-3. Finite Element Method:

Each of the previous cases are modeled using finite element method with element type (structural beam, 3D finite strain, 3 nodes 189) in ANSYS11 program. The boundary conditions of beam are simply supported as in Figure (1). Hence, a half-length of beam is used to analyze the problem. One end is considered as a fixed end (fixed all degree of freedom). The other end is simply which represent the end of the applied load as shown in Figure (2).

A ten element is used (11 node). Each element section is meshed with a fine mesh. The solution of problem has been done initially with static solution and then with buckling solution with ANSYS11 program. The resulted data is recorded as a critical buckling load for each case.

### 4. Results & Discussions:

The resulted data from the theoretical equation (Euler column formula) which include the critical buckling load is calculated for each case of beam section with the same beam length,

cross sectional area and material properties as mentioned. Those values of critical buckling load are plotted and compared with those recorded from the ANSYS11 program [Figures (3 - 9)]. Hence a good agreement has been found between the theoretical and FEM values of this force for each case of the beam section (error = 0.1- 0.3%) and the results for each beam section can be explained as follow:

#### 4-1. Hollow Circular-Section:

Increasing the thickness of circular section resulted in decreasing the critical buckling load ( $P_{cr}$ ). A sharp decreasing for ( $P_{cr}$ ) is found as the uniform increasing in thickness. Hence, the force ( $P_{cr}$ ) is (6256N) at ( $t=1\text{mm}$ ) which reduce to (404N) at ( $t=5\text{mm}$ ), or in another representation, the force decrease at a percentage of (94%) through the increasing in thickness at a percentage of (80%). This is due to the decreasing in the moment of inertia. It can be say that a thinner ring beam section gives a good buckling property than the thicker ring beam section, Figure (3).

#### 4-2. Hollow Rectangular-Section:

Variation of ( $P_{cr}$ ) with width range ( $W_1$ ), Table (1), is plotted for three values of thickness in Figure (4). As it has been shown, the critical buckling force is increase uniformly until reach the maximum value and then decrease for each thickness value. A thinner section gives a higher critical buckling load as comparing with the thicker section for each value of section width ( $W_1$ ). Increasing the width ( $W_1$ ) result in increasing the minimum moment of inertia which results in increasing ( $P_{cr}$ ) according to Eq.(8). Hence the maximum value of ( $P_{cr}=4840\text{N}$ ) is recorded at the minimum thickness ( $t=1\text{mm}$ ) and ( $W_1=25\text{mm}$ ). Therefore, this type of beam section gives a good buckling property with a thinner section.

#### 4-3. I-Section:

As in Figure (5), the critical buckling load increase with increasing the width ( $W_1$ ) for each value of thickness used in table (4), a continuous increasing is observed without decreasing. That means the maximum critical buckling load is observed at the final value of width ( $W_1$ ) used for each thickness. Where ( $P_{cr}$ )<sub>max</sub>= 4685N, at ( $t=1\text{mm}, W_1=40\text{mm}$ ), ( $P_{cr}$ )<sub>max</sub>= 1319N , at ( $t=2\text{mm} , W_1=20\text{mm}$ ) and ( $P_{cr}$ )<sub>max</sub>= 836.5N, at ( $t=3\text{mm} W_1=15\text{mm}$ ). That means, a good buckling property can be found in the thinner wide I-beam section. The narrow

thin section gives a lower ( $P_{cr}$ ). Where ( $P_{cr}$ ) is higher for ( $t=2\&3\text{mm}$ ) for width range ( $W_1 < 20\text{mm}$ ).

#### 4-4. L-Section:

Nearly, in Figure (6), the same ( $P_{cr}$ ) is observed for ( $t=2\&3\text{mm}$ ) at a width ( $W_1 < 15\text{mm}$ ) which higher than that for thickness ( $t=1\text{mm}$ ). The values of ( $P_{cr}$ ) are decrease with increasing width ( $W_1 > 20\text{mm}$ ) for ( $t=3\text{mm}$ ) and at ( $W_1 > 30\text{mm}$ ) for ( $t=2\text{mm}$ ). While, the force ( $P_{cr}$ ) is continuous in increasing with increasing width at ( $t=1\text{mm}$ ) which gives a higher values for width ( $W_1 > 30\text{mm}$ ) than those for the other thickness (2 &3mm) and reach a maximum value at the final width ( $P_{cr}=2900\text{N}$ ).

#### 4-5. T-Section:

The critical buckling load is increased gradually with width ( $W_1$ ) for to values of thickness ( $t=2\ \&3\ \text{mm}$ ) and then decreased at ( $W_1=20\ \text{mm}$ ) for thickness ( $t=3\text{mm}$ ) and at ( $W_1=30\ \text{mm}$ ) for thickness ( $t=2\text{mm}$ ). The critical buckling load is increased without decreasing for the first thickness of beam section as in Figure (7). Which gives a good buckling property as comparing with those for thickness ( $t=2\ \&3\ \text{mm}$ ) for width ( $W_1 > 34\text{mm}$ ). A wide range of width gives a good buckling property for beam section of thickness ( $t=2\text{mm}$ ) as comparing with that of thickness ( $t=3\text{mm}$ ).

#### 4-6. U-Section:

Nearly, the same critical buckling force has been shown for each set of beam section with each value of the width. This load increase gradually with width until reach the maximum value at ( $W_1=35\text{mm}$ ), ( $P_{cr})_{max}= 6522\text{N}$ , for the first set of beam section ( $t=1\ \text{mm}$ ) and then decrease, Figure (8).

#### 4-7. Z-Section:

In general, the critical buckling is increase gradually and then decrees for each set of beam thickness set during increasing the beam width. Nearly, the same value of ( $P_{cr}$ ) is found for a wide range of beam thickness set. The maximum value of ( $P_{cr}$ ) is found at ( $W_1=30\text{mm}$ ), ( $P_{cr})_{max}= 2365\text{N}$ , Figure (9).

#### 4-8. Solid-Section:

To compare the results of the above thin beam sections with those of solid sections (the same cross sectional area), the value of critical buckling force is observed ( $P_{cr} = 411N$ ) for solid square section and ( $P_{cr} = 393N$ ) for solid circle section, Table (6). Hence, a solid square section gives a good material buckling property than those of circle beam section. But a thin beam sections are a better buckling property than those of solid beam section for wide range of thickness and width. A sample of deformed and un-deformed L-beam of Figure (2b) is shown in Figure (10). The 4-mode buckling shapes for this section are shown in Figure (11).

#### 5. Conclusions:

From the previous results, it can be concluding:

- 1- A hollow thin circle and rectangular beam section gives higher critical buckling load as comparing with those of thick section.
- 2- Increasing the width of rectangular section results in increasing ( $P_{cr}$ ) until reach a maximum value and then decrease for each thickness value.
- 3- A lower critical buckling load is observed for thinner I-beam section as comparing with those of thick section for each value of beam section.
- 4- The critical buckling load increase with increasing the width of I-beam section without decreasing at any value of width or thickness of beam.
- 5- The L & T- section, the critical buckling load is continuous increasing with increasing width for the beam section thickness ( $t=1$  mm). And reach a maximum value and then decreased with increasing width for the other beam thickness ( $t=2$  &  $3$  mm).
- 6- The critical buckling load is lower for L-beam section at a thickness ( $t=1$ mm) as comparing with the other two thickness at the range of ( $W_1 < 30$ mm) and higher at the range of ( $W_1 > 30$ mm).
- 7- The critical buckling load is lower for T-beam section at a thickness ( $t=1$ mm) as comparing with the other two thickness at the range of ( $W_1 < 34$ mm) and higher at the range of ( $W_1 > 34$ mm).
- 8- Nearly, the same critical buckling load has been observed for U & Z-beam section during a wide range of width and thickness.
- 9- A solid circle or rectangular beam gives a lower buckling load than thinner section.
- 10- Changing the shape of beam section with the same area result in changing in the critical buckling load.

- 11- The maximum critical buckling load has been found in the thinner U-beam section with ( $t=1\text{mm}$  &  $W_1=35\text{mm}$ ),  $(P_{cr})_{max} = 6522\text{N}$ .
- 12- The suggested FE model in the ANSYS11 program gives good results of  $(P_{cr})$  as comparing with (Euler column formula).

## 6. REFERENCES:

- [1] A. Michalopoulos et al., "On The Buckling of Fiber-Bundle Type Beams", Jordan Journal of Civil Engineering, Vol.1, No.1, 2007.
- [2] Amir Javidinejad, Zodiac Aerospace, " Buckling of Beams and Columns Combined Axial and Horizontal Loading With Various Axial Loading Application Locations", Journal of Theoretical and Applied Mechanics, Vol. 42, No.4, 2012, pp.19-30.
- [3] Ioannis G. Raftoyiannis and Theodore Adamakos, "Critical Lateral-Torsional Buckling Moments of Steel Web-Tapered I-beams", The Open Construction and Building Technology Journal, Vol. 4, No.2, 2010, pp.105-112.
- [4] Dewey H. Hodges, David A. Peters, " Lateral-torsional buckling of cantilevered elastically coupled composite strip and I-beams", International Journal of Solids and Structures 38 (2001), pp.1585-1603.
- [5] Michael C.H. Yam et al. "The Local Web Buckling Strength of Stiffened Coped Steel I-Beams", Steel Structures 7 (2007), pp.129-138.
- [6] Goutam Saha and Sajeda Banu, "Buckling Load of A beam-Column for Different End Conditions Using Multi-Segment Integration Technique ", ARPN Journal of Engineering and Applied Sciences, Vol.2, NO. 1, February 2007.
- [7] Trahair N.S., *Flexural-Torsional Buckling of Structures*, FN Sport, London, 1993.
- [8] Wang C.M., Wang L. & Ang K., *Beam-Buckling Analysis Via Automated Rayleigh - Ritz Method*, Journal of Structures Engineering , 1994, pp. 200-211.
- [9] Ioannidis G., Marenholtz O. & Kounadis A.N., *Lateral Post-Buckling Analysis of Beams*, Archive of Applied Mechanics, 1993, pp. 151-158.
- [10] Kounadis A.N. and Ioannidis G.I., *Lateral Post-Buckling Analysis of Beam Columns*, Journal of Engineering Mechanics, 1994, pp.695-706.
- [11] Ioannidis G.I., Kounadis A.N., *Lateral Elastic Post Buckling Analysis of Elastically Rotationally Restrained I-beam Columns*, Proc. 1st European Conference on Steel Structures, Athens. 1995, pp. 41-46.

[12] Gokmen Atlihan, *Buckling Analysis of Delaminated Composite Beams*, Indian Journal of Engineering and Materials Sciences, Vol.20, August 2013, pp.276-282.

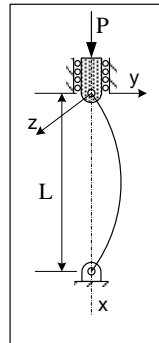
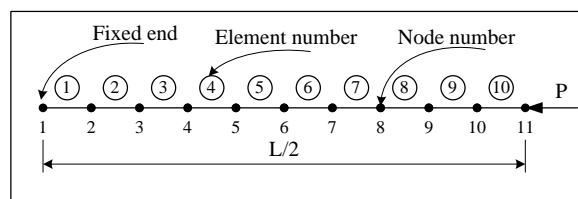
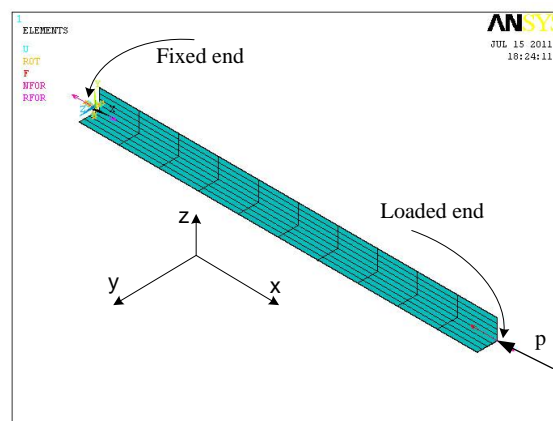


Figure (1) Buckling of pin-pin ends beam.



(a) Schematic Graph for all beam sections.



(b) ANSYS model for L-section ( $W_1=50$ ,  $W_2=51$  &  $t=1\text{mm}$ ).

Figure (2) Finite element model of half beam length with boundary conditions and the applied load.

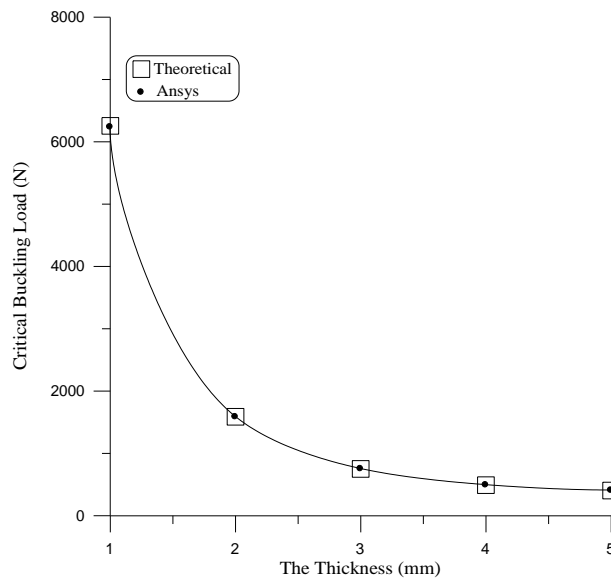


Figure (3) Variation of critical buckling load with thickness for Hollow circle-section.

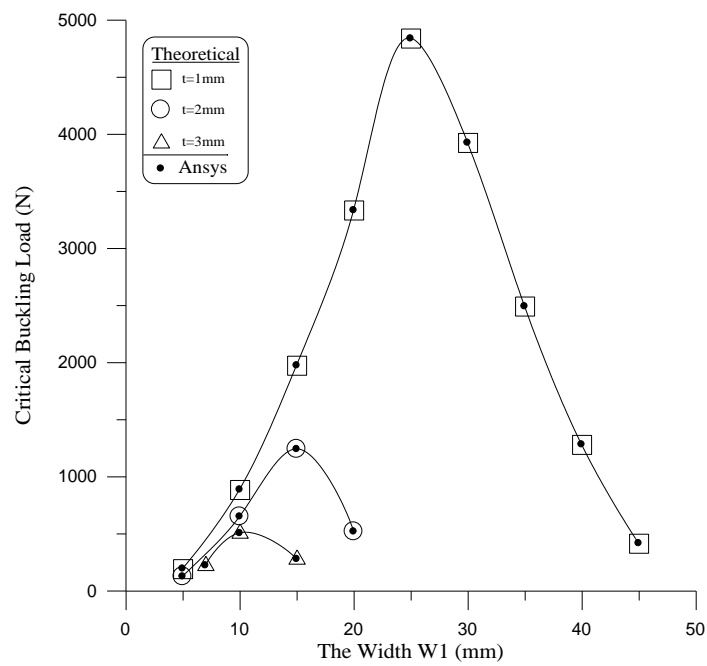


Figure (4) Variation of critical buckling load with width for Hollow rectangular-section.

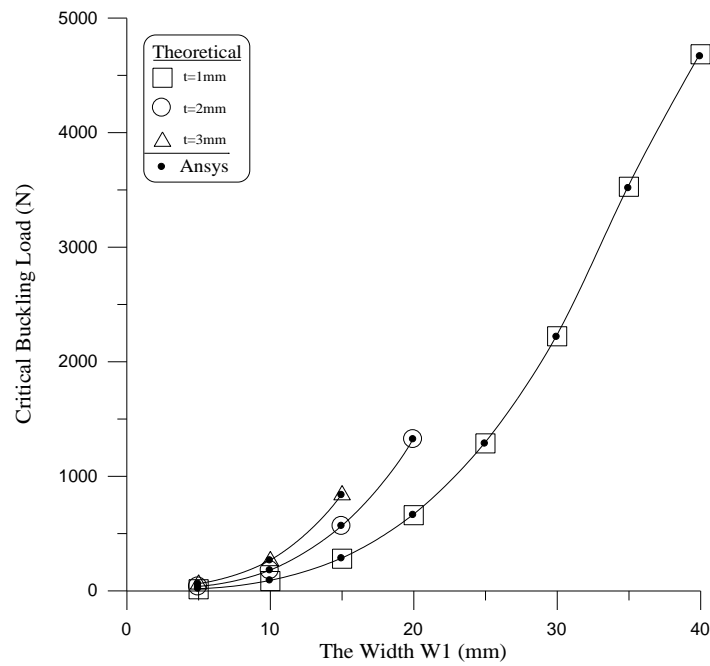


Figure (5) Variation of critical buckling load with width for I-section.

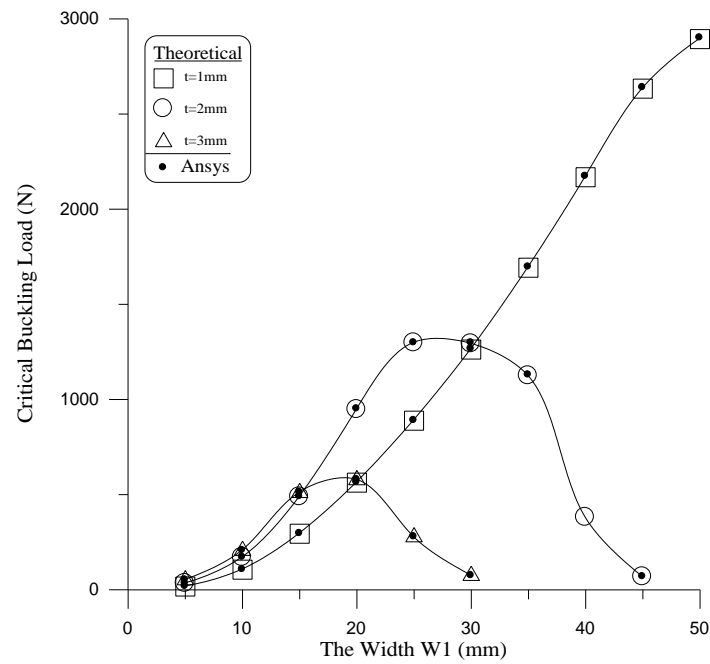


Figure (6) Variation of critical buckling load with width for L-section.



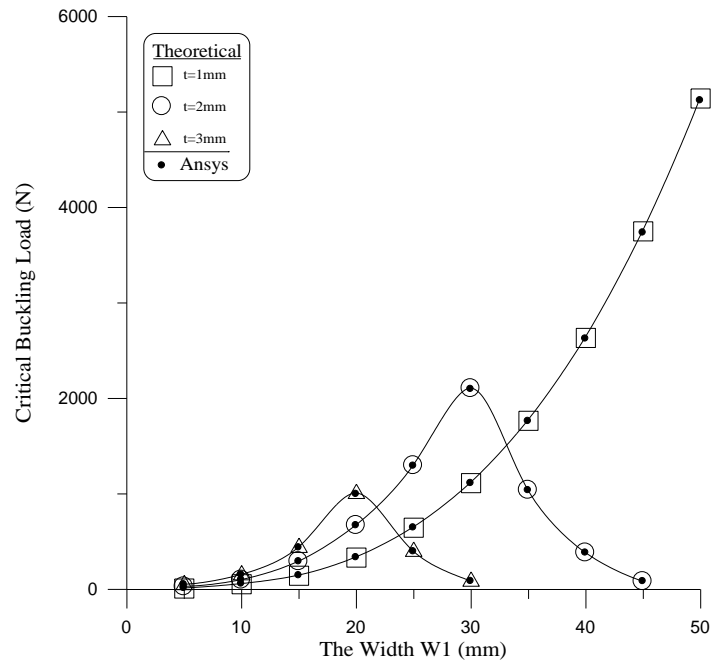


Figure (7) Variation of critical buckling load with width for T-section.

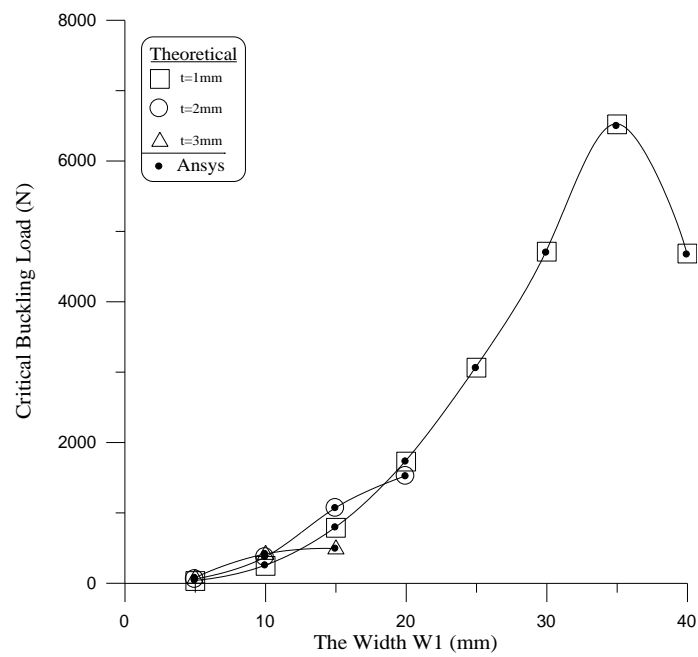


Figure (8) Variation of critical buckling load with width for U-section.

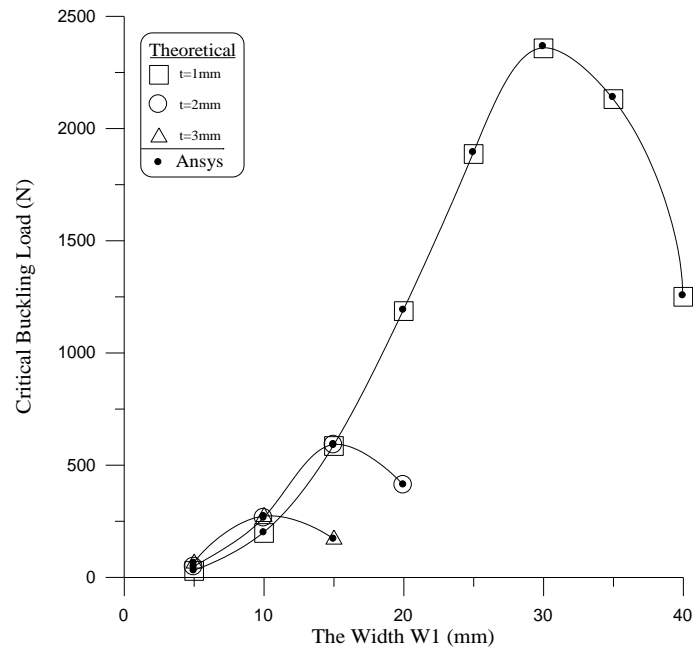
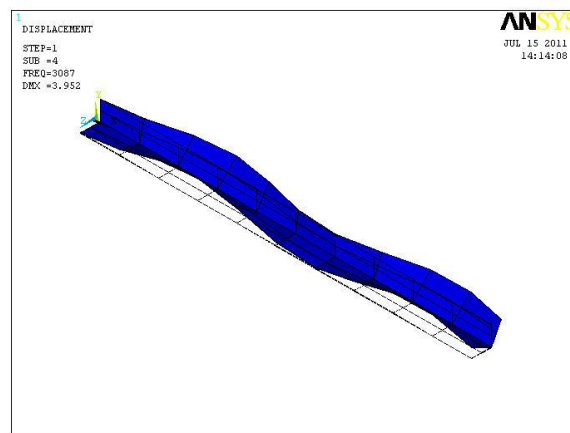
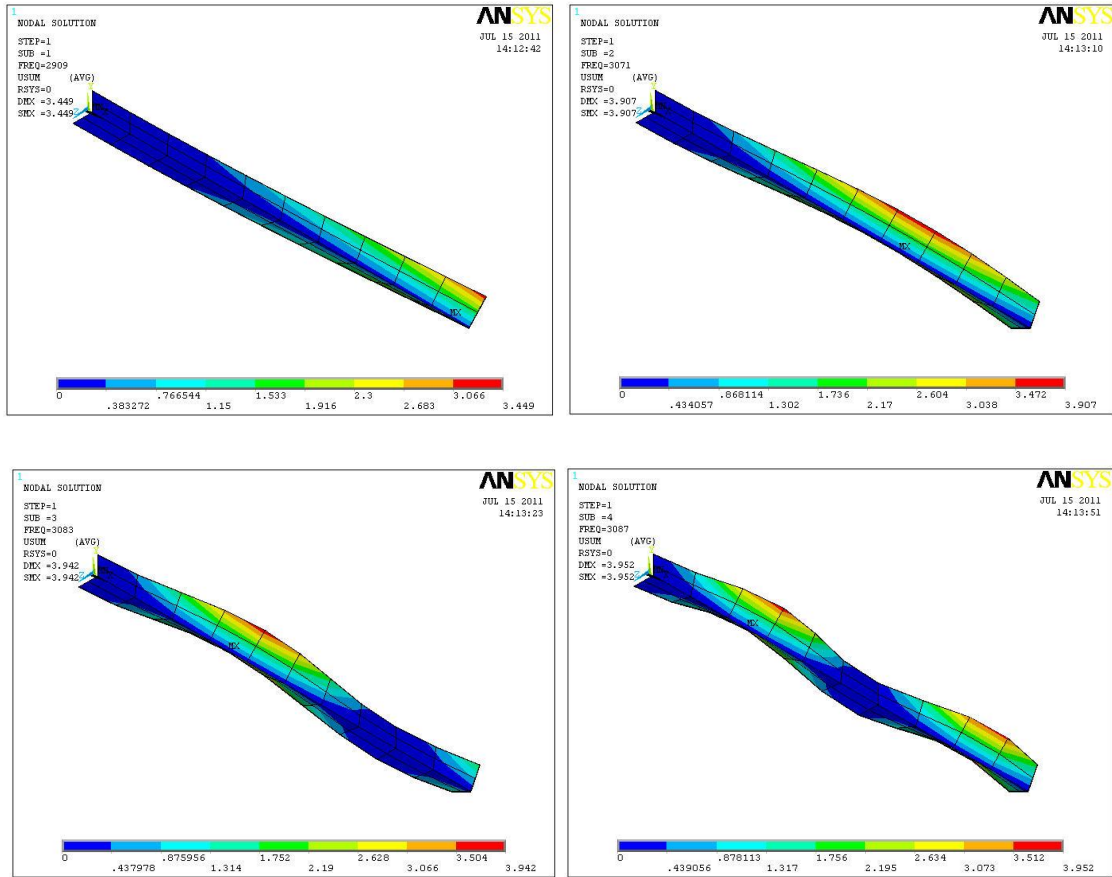


Figure (9) Variation of critical buckling load with width for Z-section.



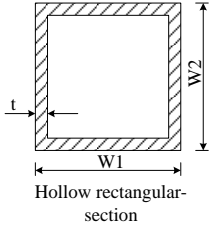
Figure(10) The deformed and un-deformed L-beam for mode shape - 4.



Figure(11) The deformed L-beam with four mode shapes.

Table (1) Dimensions of Hollow rectangular-section.

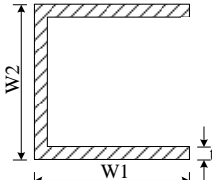
t=1mm		t=2mm		t=3mm	
W1(mm)	W2(mm)	W1(mm)	W2(mm)	W1(mm)	W2(mm)
5	47	5	24	7	15.6666
10	42	10	19	10	12.6666
15	37	15	14	15	7.66666
20	32	20	9		
25	27	25	4		
30	22				
35	17				
40	12				
45	7				
50	2				



Hollow rectangular-section

Table (2) Dimensions of channel-section.

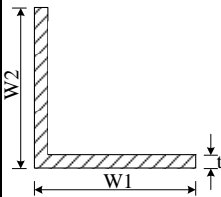
t=1mm		t=2mm		t=3mm	
W1(mm)	W2(mm)	W1(mm)	W2(mm)	W1(mm)	W2(mm)
5	92	5	44	5	29.3333
10	82	10	34	10	19.3333
15	72	15	24	15	9.3333
20	62	20	14		
25	52				
30	42				
35	32				
40	22				



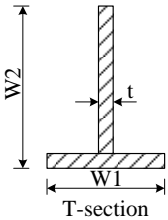
Channel-section

Table (3) Dimensions of L and T-section.

t=1mm		t=2mm		t=3mm	
W1(mm)	W2(mm)	W1(mm)	W2(mm)	W1(mm)	W2(mm)
5	96	5	47	5	31.3333
10	91	10	42	10	26.3333
15	86	15	37	15	21.3333
20	81	20	32	20	16.3333
25	76	25	27	25	11.3333
30	71	30	22	30	6.3333
35	66	35	17		
40	61	40	12		
45	56	45	7		
50	51				



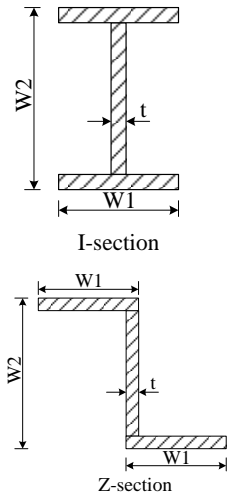
L-section



T-section

Table (4) Dimensions of I and Z-section.

t=1mm		t=2mm		t=3mm	
W1(mm)	W2(mm)	W1(mm)	W2(mm)	W1(mm)	W2(mm)
5	92	5	44	5	29.3333
10	82	10	34	10	19.3333
15	72	15	24	15	9.3333
20	62	20	14		
25	52				
30	42				
35	32				
40	22				

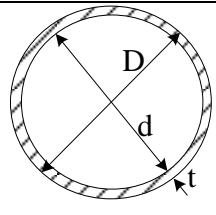


I-section

Z-section

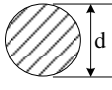
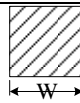
Table (5) Dimensions of Hollow Circle-Section.

t (mm)	d(mm)	D(mm)
1	30.831	32.831
2	13.915	17.915
3	7.61	13.61
4	3.9577	11.957
5	1.36	11.366



Hollow shaft-section

Table (6) Dimensions of Solid Circle and Square-Section.

<b>d=11.2837 mm</b>	 Solid circle-section
<b>W=10mm</b>	 Solid square-section